$CH(X^2\Pi, a^4\Sigma^-)\ldots OH_2$ and $CH_2(\tilde{X}^3B_1, \tilde{a}^1A_1)\ldots OH_2$ Interactions. A First Principles Investigation

DEMETER TZELI, ARISTIDES MAVRIDIS

Department of Chemistry, Laboratory of Physical Chemistry, National and Kapodistrian University of Athens, P. O. Box 64 004, 157 10 Zografou, Athens, Greece

ABSTRACT: We have investigated the interaction of the methylidene, $CH(X^2\Pi, a^4\Sigma^-)$ and methylene, $CH_2(\tilde{X}^3B_1, \tilde{a}^1A_1)$ with H_2O, employing the (P)MPn ($n = 2, 4$) techniques in conjunction with the sequence of correlation consistent basis sets aug-cc-pVxZ, $x = 2, 3$, and 4. For the $CH\ldots OH_2$ system, we have located four minima (m) and three transition states (ts) and for the $CH_2\ldots OH_2$, five minima and four transition states. All our results have been corrected for zero-point energy (ZPE) and basis set superposition errors (BSSE), while for the most important m_ structures, we report complete basis set (CBS) interaction limits. We also report fully optimized geometries, harmonic frequencies, dipole moments, Mulliken charges, and potential energy curves. The highest $CH(X^2\Pi)\ldots OH_2$ (m1_$^2\Pi$) and $CH_2(\tilde{a}^1A_1)\ldots OH_2$ (m1_$^1A_1$) interactions are the result of electron transfer from the oxygen atom to the empty p_π orbitals of $CH(X^2\Pi)$ and $CH_2(\tilde{a}^1A_1)$, respectively (ylide-like structures). At the (P)MP4/AQZ//MP2/ATZ level, including ZPE, BSSE, and CBS extrapolation, we obtain $\Delta E_0(BSSE)+CBS = -9.36$ kcal/mol at $r_{C\ldots O} = 1.752$ Å, and -9.73 kcal/mol at $r_{C\ldots O} = 1.741$ Å for the m1_$^2\Pi$ and m1_$^1A_1$, respectively.   © 2005 Wiley Periodicals, Inc. Int J Quantum Chem 104: 497–511, 2005

Key words: ab initio calculations; methylidene–water; CH–H$_2$O; methylene–water; CH$_2$–H$_2$O; van der Waals interactions

Introduction

Ylides are reactive intermediates that undergo synthetically useful transformations, defined as compounds in which a positively charged atom from group 15 (VA) or 16 (VIA) of the periodic table is connected to a carbon atom carrying an unshared pair of electrons [1]. One method of synthesizing this class of compounds is by the interaction of carbenes with a nucleophile related to elements of group 15 or 16. For instance, in a well-known textbook of organic chemistry [2], the structure of prototypical nitrogen ylide is written as R_3N^+–CH_2^-. During the past two decades, there has been a

growing interest in the use of carbonyl ylides for the synthesis of oxygenated heterocycles (see Ref. [1] and references therein).

Now, methylidene, CH ($X^2\Pi$) is one of the simplest and most reactive radicals, and it is believed to play an important role in atmospheric chemistry. Experimental work on the reaction of CH with small molecules such as N_2, NO, N_2O, CO, CO_2, and H_2O [3–5] and computational work on the reaction CH ($X^2\Pi$ or $a^4\Sigma^-$) + H_2O [6–8] have been reported in the literature.

The parental carbene CH_2 ($\tilde{X}^3B_1$), perhaps the most famous molecule in the evolution of computational quantum chemistry [9], is an important intermediate, also playing a significant role in planetary atmosphere. The reaction of CH_2 ($\tilde{a}^1A_1$) with H_2O producing CH_3OH through an ylide-like intermediate, has been experimentally studied by mass spectrometric techniques [10]. Furthermore, the reactions CH_2 ($\tilde{a}^1A_1$) + $H_2O \rightarrow CH_2$ ($\tilde{X}^3B_1$) + H_2O and CH_2 ($\tilde{a}^1A_1$) + $H_2O \rightarrow CH_3$ + OH, the formation of methanol and of formaldehyde, have been investigated with laser-induced fluorescence detection under quasi-stationary and first order conditions [11, 12], while the first of the reactions above was also studied by laser flash photolysis/laser absorption methods [13].

The first computational work on the system $CH_2(\tilde{a}^1A_1)\ldots OH_2$ was done in 1980 by Harding et al. [14], where they calculated two minima, and in 1981 by Eades et al. [15], who calculated the three lowest configurations corresponding to two minima and one transition state. In the following years, the global minimum [16–20], the second minimum [21], the third minimum [19], and a transition structure [19] were studied. Previous theoretical work on the $CH\ldots OH_2$, $CH_2\ldots OH_2$ systems is summarized in Table I.

In the present report, we undertake a systematic study of the interaction of CH ($X^2\Pi$, $a^4\Sigma^-$), CH_2 ($\tilde{X}^3B_1$, $\tilde{a}^1A_1$) with H_2O, using Møller–Plesset (MP) perturbation theory and relatively large basis sets. We report fully optimized geometries, interaction energies, harmonic frequencies, dipole moments and Mulliken charges, trying at the same time to understand the $CH\ldots OH_2$, and $CH_2\ldots OH_2$ interaction mechanisms.

Methodological Details

The $CH\ldots OH_2$, $CH_2\ldots OH_2$ calculations were performed using, for all atoms, the augmented cor-

relation consistent series of basis sets, aug-cc-pVxZ (AxZ), x = 2(D), 3(T), 4(Q) of Dunning and coworkers [22]. The interaction between (CH, CH_2) + H_2O is such (vide infra) that there is no need for a multireference approach. Therefore, we have used the single reference MP perturbation theory, MP2 and MP4, for the singlets, and UMP2, UMP4, PMP2, and PMP4 for the doublets, triplets, and quartets, as implemented in the Gaussian 94 [23a] and Gaussian 98 [23b] suite of codes. All structures were fully optimized at the above correlated levels, with the exception of UMP4/ATZ and UMP2, UMP4/AVQZ, where single point calculations were performed at the (U)MP2/ATZ geometry. The "very tight" option of the program was used, while the energies were converged to ~0.01 μE_h with corresponding root mean square (rms) deviation of the energy gradient with respect to nuclear coordinates of 11 μE_h/bohr. Harmonic frequencies were calculated for all structures at the (U)MP2/(ADZ, ATZ) level of theory. Spin contamination of the UMP calculations is not alarming: the $\langle S^2 \rangle$ values range from 0.7596 to 0.7711 (instead of 0.75) for the doublets, 2.0156 to 2.0161 (instead of 2.0) for the triplets, and 3.7540 to 3.7544 (instead of 3.75) for the quartets.

Because of the importance of basis set superposition error (BSSE) [24] in weakly or van der Waals interacting systems [25], the interaction energies were BSSE corrected [26]. The interaction energy ΔE of a XY van der Waals molecule and the corresponding BSSE corrected value Δ(BSSE) are defined as follows [27]:

$$\Delta E = E_{XY}^{xy}(XY) - E_X^x(X) - E_Y^y(Y) \qquad (1)$$

$$\Delta E(BSSE) = E_{XY}^{xy}(XY) - E_{XY}^{xy}(X) - E_{XY}^{xy}(Y) + E_{XY}^x(X)$$
$$- E_X^x(X) + E_{XY}^y(Y) - E_Y^y(Y), \quad (2)$$

where $E_G^S(M)$ refers to the total energy of molecule M at the geometry G computed with basis set s. Within the method employed, relation (1) needs no correction with respect to basis set size for "infinitely" large, i.e., complete basis sets (CBS). We also recall that the MP approach is size-extensive, a particularly useful property in the present study. CBS limits were obtained by applying the simple exponential formula $P(x) = P(\infty) + Ae^{-Bx}$, where P is a generic property; n reflects the quality of the basis set; x = 2, 3, and 4; and A, B are freely adjustable parameters [28]. Finally, all our calculations are valence-correlated, i.e., the ~$1s$ carbon

TABLE I

Previous theoretical work on CH . . . OH_2 and CH_2 . . . OH_2 systems.*

Method	E (hartree)	$\{r\}$[b]	$\Delta E(\Delta E_0)$
	CH . . . OH_2		
m1_$^2\Pi$			
UMP2/6-31G**[c]	−114.59632	1.868	−14.3 (−12.0)
MP2/6-31G(d′) (=A)[d,e]	−114.562765	1.832	−15.3
QCISD(T)/6-31G(d′)//A[d,e]	−114.613477		−12.3
MP4(SDQ)/CBSB4//A[d,e]	−114.641734		−8.5
CBS-Q (0 K)// A[d,e]	−114.763895		−9.6
m2_$^2\Pi$[b]			
MP2/6-31G(d′) (=A)[d]	−114.545255	2.320	−4.3
QCISD(T)/6-31G(d′)// A[d]	−114.599747		−3.6
MP4(SDQ)/CBSB4// A[d]	−114.633612		−3.4
CBS-Q (0 K)// A[d]	−114.751696		−1.9
ts2_$^2\Pi$[b]			
MP2/6-31G(d′) (=**A**)[d,f]	−114.539180	2.409	−0.5
QCISD(T)/6-31G(d′)//A[d,f]	−114.597846		−2.5
MP4(SDQ)/CBSB4//A[d,f]	−114.625735		+1.5
CBS-Q (0 K)//A[d,f]	−114.751008		−1.5
	CH_2 . . . OH_2		
m1_$^1A_1$			
RMP2/6-31G**//RMP2/6-31G*[g]	−115.23560	1.805	−18.1
RMP4/6-31G**//RMP2/6-31G*[g]	−115.26205		−14.7
HF/dz+(sd-diff,C / d-pol C,O)[h]		1.825	a+1.0
MP4(SDQ)/6-31G**(=B)//HF/B[i]	−115.25956		−13.44
UMP2/6-31G* (=C)[j]	−115.20329	1.805	−18.85
UMP2/6-311G(df,p)//C[j]	−115.33007		−20.14
UMP4/6-31G**//C[j]	−115.26944		−16.53
CAS/CCI/aug-pol-dz[k]	−115.37254	2.366	−7.62 (−4.60)
CCI+Q/ aug-pol-dz[k]	−115.40517		−8.95 (−5.93)
CAS/CCI/tz-double pol[k]	−115.36931		−5.91 (−2.89)
CCI+Q/tz-double pol[k]	−115.40561		−9.54 (−6.52)
MP2/6-31G*[l]	−115.203286		−18.8 (−12.8)
MP2/6-311G**[l]	−115.335146	1.77	−18.7 (−12.8)
MP2/6-311++G**[m]		1.758	(−9.57)
QCISD/6-311++G**[m]		1.874	(−6.53)
B3LYP/6-31G*[m]		1.866	(−15.26)
B3LYP/6-311++G**[m]		1.857	(−10.52)
ts1_$^1A_1$			
HF/dz + (sd-diff,C/d-pol C,O)[h]		—	a+5.6
m2_$^1A_1$[b]			
HF/dz + (sd-diff,C/d-pol C,O)[h]		1.870	a
MP2/6-311++G** (=E)[n]		1.778	(−9.30)
QCISD/6-311++G**[n]		1.883	(−5.02)
QCISD(T)/E//QCISD/E[n]			(−6.37)
m3_$^1A_1$			
RMP2/6-31G**//RMP2/6-31G*[g]	−115.21753	2.153	−6.7
RMP4/6-31G**//RMP2/6-31G*[g]	−115.24829		−6.4
MP2/6-31G*[l]	−115.184626		−7.1 (−4.7)
MP2/6-311G**[l]	−115.314750	2.17	−5.9 (−3.8)
ts3_$^1A_1$			
MP2/6-31G*[l]	−115.177624	2.49	−2.7 (−1.6)

* Total energies E (hartree), van der Waals distances r(Å), interaction energies ΔE and $\Delta E_0 = \Delta E + ZPE^a$ (kcal/mol).

[a] Zero-point energy.
[b] van der Waals distances (see Figs. 1 and 2).
[c] Ref. [6].
[d] Ref. [7].
[e] It is reported that this structure is metastable rearranging to a more stable product, but our calculations show that it is minimum.
[f] This structure is reported as minimum, but our calculations show that it is a transition state.
[g] Ref. [14].
[h] Ref. [15].
[i] Ref. [16].
[j] Ref. [17].
[k] Ref. [18].
[l] Ref. [19].
[m] Ref. [20].
[n] Ref. [21].

TABLE II

Absolute energies E (hartree), geometries r_e(Å), θ_e (degrees), and energy gaps T_e (kcal/mol) of CH, CH_2, and H_2O molecules at different levels of theory.

Method	E	r_e	θ_e	E	r_e	θ_e	T_e
				CH			
		$X^2\Pi$			**$a^4\Sigma^-$**		
				ADZ			
UMP2	−38.358393	1.1298		−38.345542	1.0964		8.06
PMP2	−38.359975			−38.345943			8.80
UMP4	−38.383523	1.1385		−38.361737	1.1041		13.67
PMP4	−38.384378			−38.361995			14.05
				ATZ			
UMP2	−38.385000	1.1193		−38.368787	1.0820		10.17
PMP2	−38.386724			−38.369209			10.99
UMP4	−38.409177	1.1207		−38.384774	1.0882		15.31
PMP4	−38.410075			−38.385033			15.71
				AQZ			
UMP2	−38.393390	1.1117		−38.375593	1.0807		11.17
PMP2	−38.395128			−38.376020			11.99
UMP4	−38.416010	1.1191		−38.390731	1.0868		15.86
PMP4	−38.416904			−38.390989			16.26
Expt		1.1197868[a]			1.0977[b]		17.1(2)[c]
				CH_2			
		$\tilde{X}^3B_1$			**$\tilde{a}^1A_1$**		
				ADZ			
UMP2	−39.025270	1.0883	132.61	−38.999960	1.1195	101.51	15.88
PMP2	−39.027095						17.03
UMP4	−39.046594	1.0928	132.89	−39.027539	1.1268	100.75	11.96
PMP4	−39.047734						12.64
				ATZ			
UMP2	−39.057582	1.0741	132.93	−39.034412	1.1045	102.09	14.54
PMP2	−39.059461						15.72
UMP4	−39.078403	1.0778	133.41	−39.060791	1.1108	101.44	11.05
PMP4	−39.079535						11.76
				AQZ			
UMP2	−39.066894	1.0725	133.02	−39.044750	1.1027	102.22	13.90
PMP2	−39.068783						15.08
UMP4	−39.086372	1.0762	133.47	−39.069253	1.1090	101.57	10.74
PMP4	−39.087497						11.45
Expt		1.0753(3)[d]	133.93(1)		1.111[e]	102.4	9.12(6)[f]
							9.023(14)[g]
		H_2O					
		ADZ					
MP2	−76.260909	0.9659	103.87				
MP4	−76.274512	0.9670	103.88				
		ATZ					
MP2	−76.328992	0.9614	104.11				
MP4	−76.343678	0.9627	104.06				
		AQZ					
MP2	−76.351919	0.9589	104.27				
MP4	−76.365085	0.9601	104.24				
Expt		0.9587(1)[h]	103.89(6)				
		0.95748(2)[i]	105.019(13)				
		0.9572(3)[j]	104.52				

[a] Expt., Ref. [29b].
[b] Ref. [29c], r_0.
[c] Ref. [29d], T_0.
[d] Ref. [30c].
[e] Ref. [30a].
[f] Ref. [30d].
[g] Ref. [30e].
[h] Ref. [31a].
[i] Ref. [31b].
[j] Ref. [31c].

TABLE III

Harmonic frequencies ω(cm^{-1}) and zero-point energies (ZPE) (kcal/mol) of CH($X^2\Pi$, $a^4\Sigma^-$), CH$_2$($\tilde{X}^3B_1$, $\tilde{a}^1A_1$), and H$_2$O($\tilde{X}^1A_1$) molecules at the (U)MP2/AxZ, x = D, T, Q level of theory.*

	ADZ	ATZ	AQZ	Expt	ADZ	ATZ	AQZ	Expt/Theory
			CH($X^2\Pi$)				CH($a^4\Sigma^-$)	
ω_e	2930	2948	2956	2860.75[a]	3193	3206	3209	3090.9[b]
ZPE	4.188	4.214	4.227	4.090[a]	4.565	4.583	4.587	4.419[b]
			CH$_2$($\tilde{X}^3B_1$)				CH$_2$($\tilde{a}^1A_1$)	
ω_1	1138	1132	1134		1408	1471	1420	
ω_2	3183	3199	3205		2975	2991	2997	
ω_3	3420	3432	3441		3056	3067	3078	
ZPE	11.07	11.10	11.12	10.683[c]	10.64	10.69	10.71	10.327[c]
			H$_2$O($\tilde{X}^1A_1$)					
ω_2 (a_1)	1622	1628	1632	1648[d]				
ω_1 (a_1)	3803	3822	3840	3832[d]				
ω_3 (b_2)	3938	3948	3966	3943[d]				
ZPE	13.39	13.44	13.49	13.47[d]				

* Experimental or very accurate theoretical values are also given.
[a] Ref. [29b].
[b] Accurate theoretical values (Ref. [32]).
[c] Expt. Ref. [30g].
[d] Ref. [31c].

and oxygen orbitals were always kept doubly occupied.

CH, CH$_2$, and H$_2$O Molecules

Total energies, geometries, and harmonic frequencies of CH($X^2\Pi$, $a^4\Sigma^-$), CH$_2$($\tilde{X}^3B_1$, $\tilde{a}^1A_1$), and H$_2$O($\tilde{X}^1A_1$) molecules are reported in Tables II and III. At the highest level of calculation, (U)MP4/AQZ, the geometries of all three molecules are in very good agreement with the experiment [29–31]. The energy gap $a^4\Sigma^- \leftarrow X^2\Pi$ of CH is T_0 = 16.2 (16.6) kcal/mol at the UMP4(PMP4)/AQZ level (where P stands for "projected"), in fair agreement with the experimental value of 17.11 ± 0.18 kcal/mol [29c, 29d]. The same can be said for the energy separation $\tilde{a}^1A_1 \leftarrow \tilde{X}^3B_1$ of CH$_2$, where at the (U)MP4[(P)MP4)]/AQZ level, we obtain T_0 = 10.3 [11.0] kcal/mol, as compared with the experimental value, T_0 = 8.998 ± 0.014 kcal/mol [30f]. Here, zero-point energies (ZPE) have been calculated at the (U)MP2/AQZ level (Table III), admittedly not in very good agreement with experiment (or best ab initio values), but fair enough for the purposes of the present work.

Now, and for reasons that will be useful in the following sections, we give the valence–bond–

Lewis (vbL) diagrams of all species involved in this work [Schemes (1)–(5); see also Refs. [9] and [32]).

From these icons, it is clear that, in general, the interaction energies of CH($X^2\Pi$) and CH$_2$($\tilde{a}^1A_1$) with H$_2$O, should be much larger than the corresponding interactions of CH($a^4\Sigma^-$) and CH$_2$($\tilde{X}^3B_1$) + H$_2$O. "Bonding" in the first pair with water is plausible through an electron transferring mechanism to the available $2p_x$ and $2p_{x,y}$ orbitals of CH($X^2\Pi$) and CH$_2$($\tilde{a}^1A_1$) respectively, but shut off in the CH($a^4\Sigma^-$), CH$_2$($\tilde{X}^3B_1$) pair.

Results and Discussion

CH ... H$_2$O

We have calculated four structures of the CH($X^2\Pi$) ... OH$_2$ complex, as shown in Figure 1, two minima (m) and two transition states (ts), and three CH($^4\Sigma^-$) ... OH$_2$ structures (two m and one ts). Table IV presents absolute energies, BSSE-corrected dissociation energies ΔE(BSSE), ΔE_0(BSSE) = ΔE(BSSE) + ZPE corrections; CBS limits are also given for the m1_$^2\Pi$, m2_$^2\Pi$, and m1_$^4\Sigma^-$ species. Tables V and VI list ZPEs, harmonic frequencies (ω_e), Mulliken charges, and dipole moments (μ) respectively.
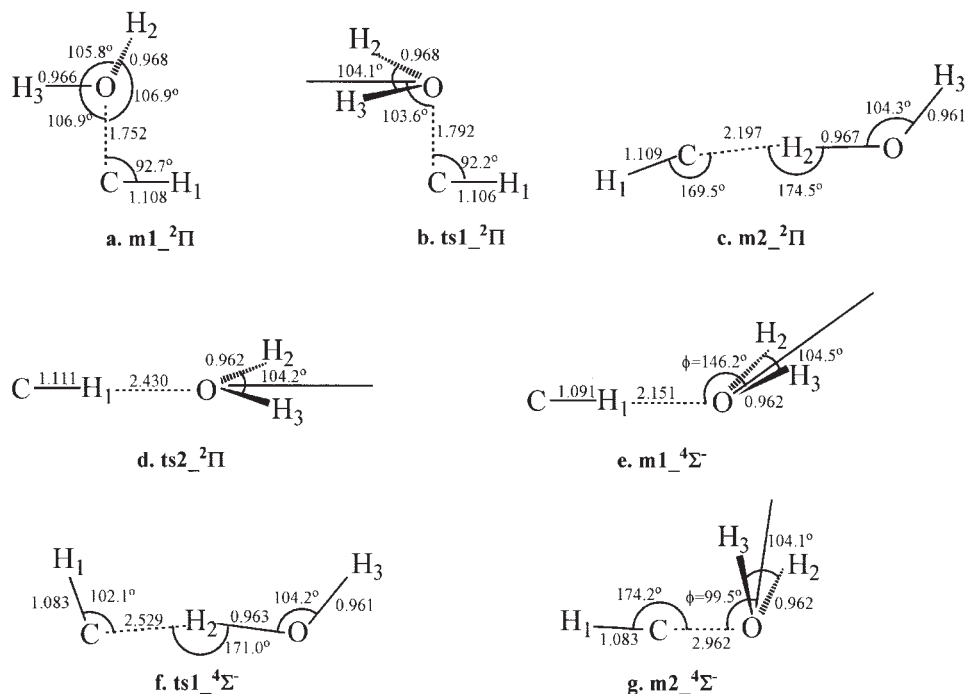
FIGURE 1. Geometries of the CH($^2\Pi$) . . . OH$_2$ and CH($^4\Sigma^-$) . . . OH$_2$ minima. Bond distances in Å at the UMP2/ATZ level.

At the PMP4/AQZ-CBS level, the interaction energy of m1_$^2\Pi$ (global minimum, C$_1$) is ΔE(BSSE) = -13.7 kcal/mol, or ΔE_0(BSSE) = -9.36 kcal/mol, using the ATZ–ZPE corrections. The interaction takes place by charge transfer from the water oxygen atom to the empty $2p_x$ orbital of the CH(X$^2\Pi$) state, Scheme (1), forming an ylide-like complex at $r_{C...O} = 1.752$ Å (Fig. 1). Corresponding literature results at the UMP2/6-31G** [6] and UMP2/6-31G* (d) [7] are $\Delta E = -14.3$ kcal/mol, $r_{C...O} = 1.868$ Å, and -15.3 kcal/mol, $r_{C...O} = 1.832$ Å, respectively.

However, no BSSE corrections have been applied in Ref. [6], while the results reported by Jursic [7] lack both ZPE and BSSE corrections. At the UMP4(SDQ)/CBSB4//UMP2/6-31G* (d) level, Jursic gives $\Delta E = -8.5$ kcal/mol. It is interesting that correcting the ΔE value of Jursic [7] for ZPE and BSSE at the UMP4(SDTQ)/ADZ level (slightly better than that of Ref. [7]), using our results (Table IV), one obtains $\Delta E = -8.5 + 4.1 + 2.1 = -2.3$
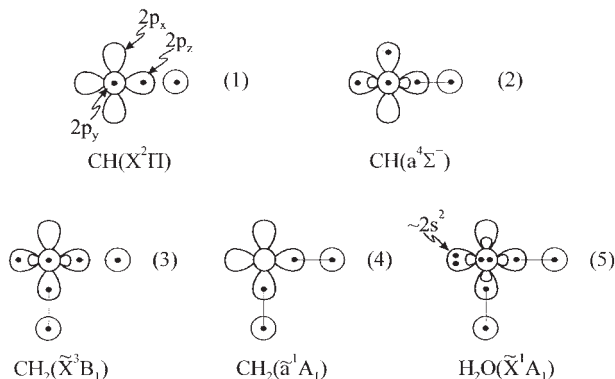
SCHEMES 1–5.
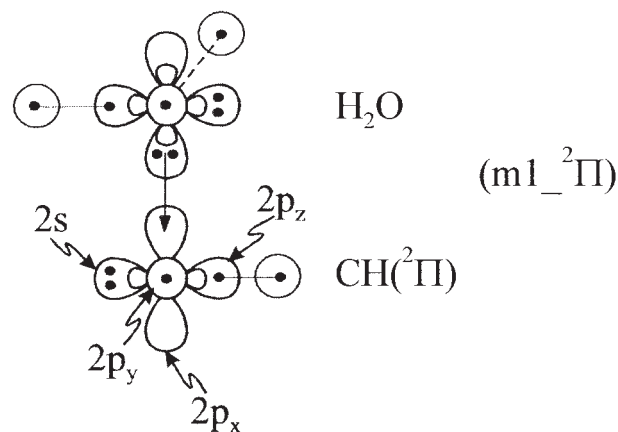
SCHEME 6.

TABLE IV

Total energies E (hartree), interaction energies ΔE (kcal/mol), basis set superposition error-corrected ΔE, ΔE(BSSE) (kcal/mol), and zero-point energy-corrected ΔE(BSSE), ΔE_0(BSSE) (kcal/mol), of CH($X^2\Pi$, $a^4\Sigma^-$) . . . OH_2 complexes at different levels of theory.

	E	ΔE	ΔE(BSSE)	ΔE_0(BSSE)	E	ΔE	ΔE(BSSE)	ΔE_0(BSSE)
				ADZ				
			UMP2				**UMP4**	
m1_$^2\Pi$	−114.63898	−12.35	−10.19	−6.13	−114.67625	−11.43	−9.35	−5.28
ts1_$^2\Pi$	−114.63862	−12.12	−10.04	−6.32	−114.67607	−11.32	−9.30	−5.58
m2_$^2\Pi$	−114.62543	−3.84	−3.23	−1.62	−114.66386[a]	−3.65	−3.04	−1.43
ts2_$^2\Pi$	−114.62245	−1.97	−1.53	−0.66	−114.66104[a]	−1.89	−1.44	−0.57
m1_$^4\Sigma^-$	−114.61141	−3.11	−2.51	−1.04	−114.64161	−3.36	−2.68	−1.21
ts1_$^4\Sigma^-$	−114.60806	−1.01	−0.56	+0.21	−114.63801[a]	−1.11	−0.64	+0.13
m2_$^4\Sigma^-$	−114.60778	−0.84	−0.47	+0.51	−114.63784[b]	−1.00	−0.60	+0.38
			PMP2				**PMP4**	
m1_$^2\Pi$	−114.64143	−12.89	−10.72	−6.65	−114.67819	−12.11	−10.02	−5.95
ts1_$^2\Pi$	−114.64111	−12.69	−10.60	−6.87	−114.67625	−12.03	−10.01	−6.28
m2_$^2\Pi$	−114.62703	−3.86	−3.24	−1.63	−114.66473	−3.66	−3.05	−1.44
ts2_$^2\Pi$	−114.62402	−1.97	−1.52	−0.65	−114.66190	−1.89	−1.44	−0.57
m1_$^4\Sigma^-$	−114.61181	−3.11	−2.51	−1.04	−114.64187	−3.37	−2.68	−1.22
ts1_$^4\Sigma^-$	−114.60846	−1.01	−0.56	+0.21	−114.63826	−1.11	−0.64	+0.13
m2_$^4\Sigma^-$	−114.60816	−0.82	−0.45	+0.53	−114.63809	−0.99	−0.60	+0.38
				ATZ				
			UMP2				**UMP4**[c]	
m1_$^2\Pi$	−114.73595	−13.78	−12.84	−8.52	−114.77303	−12.66	−11.76	−7.44
ts1_$^2\Pi$	−114.73539	−13.43	−12.43	−8.52	−114.77272	−12.47	−11.58	−7.66
m2_$^2\Pi$	−114.72038	−4.01	−3.68	−1.97	−114.75899	−3.85	−3.54	−1.82
ts2_$^2\Pi$	−114.71712	−1.96	−1.73	−0.96	−114.75588	−1.90	−1.68	−0.91
m1_$^4\Sigma^-$	−114.70254	−2.99	−2.54	−1.10	−114.73354	−3.19	−2.89	−1.46
ts1_$^4\Sigma^-$	−114.69926	−0.93	−0.73	+0.05	−114.73009	−1.03	−0.83	−0.05
m2_$^4\Sigma^-$	−114.69900	−0.76	−0.56	+0.40	−114.72997	−0.95	−0.75	+0.22
			PMP2				**PMP4**	
m1_$^2\Pi$	−114.73853	−14.31	−13.38	−9.06	−114.77485	−13.24	−12.34	−8.02
ts1_$^2\Pi$	−114.73802	−14.00	−13.01	−9.09	−114.77463	−13.10	−12.22	−8.30
m2_$^2\Pi$	−114.72213	−4.02	−3.69	−1.98	−114.75990	−3.86	−3.54	−1.83
ts2_$^2\Pi$	−114.71883	−1.95	−1.73	−0.96	−114.75677	−1.90	−1.68	−0.91
m1_$^4\Sigma^-$	−114.70295	−2.98	−2.53	−1.10	−114.73380	−3.19	−2.89	−1.46
ts1_$^4\Sigma^-$	−114.69968	−0.93	−0.73	+0.05	−114.73035	−1.03	−0.83	−0.05
m2_$^4\Sigma^-$	−114.69940	−0.75	−0.55	+0.42	−114.73022	−0.95	−0.74	+0.23
				AQZ[d]				
			UMP2				**UMP4**	
m1_$^2\Pi$	−114.76767	−14.03	−13.52	−9.20	−114.80178	−12.98	−12.60	−8.28
CBS[e]			−13.77 ± 0.02				−13.07 ± 0.03	
m2_$^2\Pi$	−114.75158	−3.94	−3.77	−2.06	−114.78710	−3.77	−3.64	−1.93
CBS[e]			−3.80				−3.68	
m1_$^4\Sigma^-$	−114.73219	−2.93	−2.79	−1.36	−114.76078	−3.12	−3.00	−1.57
CBS[e]							−3.12 ± 0.01	
			PMP2				**PMP4**	
m1_$^2\Pi$	−114.77026	−14.56	−14.06	−9.74	−114.80360	−13.56	−13.19	−8.87
CBS[e]			−14.30 ± 0.02				−13.68 ± 0.03	
m2_$^2\Pi$	−114.75334	−3.95	−3.78	−2.07	−114.78800	−3.78	−3.65	−1.94
CBS[e]			−3.81				−3.68	
m1_$^4\Sigma^-$	−114.73219	−2.93	−2.79	−1.36	−114.76104	−3.12	−3.00	−1.57
CBS[e]							−3.12 ± 0.01	

[a] UMP4(SDTQ)/ADZ//UMP4(SDQ)/ADZ.
[b] UMP4(SDTQ)/ADZ//UMP2/ADZ.
[c] UMP4(SDTQ)/ATZ//UMP2/ATZ.
[d] UMP2, UMP4(SDTQ)/AQZ//UMP2/ATZ.
[e] Complete basis set limit (see text).

TABLE V _____

UMP2/ATZ harmonic vibrational frequencies $\omega(cm^{-1})$ and zero-point energies (ZPE) (kcal/mol) of the $CH(X^2\Pi) \ldots OH_2$ (m1, ts1, m2, ts2) and $CH(a^4\Sigma^-) \ldots OH_2$ (m1, ts1, m2) complexes.

			$CH(^2\Pi) \ldots OH_2$					
m1_$^2\Pi$		**ts1_$^2\Pi$**		**m2_$^2\Pi$**		**ts2_$^2\Pi$**	
ω_1	213	ω_1 (a″)	159i	ω_1 (a′)	131	ω_1 (a′)	19.6i
ω_2	411	ω_2 (a′)	399	ω_2 (a″)	155	ω_2 (a″)	62.6
ω_3	634	ω_3 (a″)	646	ω_3 (a′)	156	ω_3 (a′)	104
ω_4	687	ω_4 (a′)	650	ω_4 (a′)	287	ω_4 (a′)	113
ω_5	1230	ω_5 (a′)	1169	ω_5 (a″)	520	ω_5 (a″)	233
ω_6	1623	ω_6 (a′)	1632	ω_6 (a′)	1641	ω_6 (a′)	1631
ω_7	2968	ω_7 (a′)	2991	ω_7 (a′)	2995	ω_7 (a′)	2983
ω_8	3743	ω_8 (a′)	3747	ω_8 (a′)	3743	ω_8 (a′)	3818
ω_9	3863	ω_9 (a″)	3851	ω_9 (a′)	3915	ω_9 (a″)	3942
ZPE	21.98	**ZPE**	21.57	**ZPE**	19.36	**ZPE**	18.422
m1_$^4\Sigma^-$		**ts1_$^4\Sigma^-$**		**m2_$^4\Sigma^-$**			
ω_1 (a′)	103.1	ω_1 (a″)	84.0i	ω_1 (a″)	69.1		
ω_2 (a″)	114.8	ω_2 (a′)	79.9	ω_2 (a′)	74.0		
ω_3 (a′)	138.2	ω_3 (a′)	101.8	ω_3 (a′)	85.9		
ω_4 (a′)	351.6	ω_4 (a″)	196.4	ω_4 (a′)	230.5		
ω_5 (a″)	420.5	ω_5 (a′)	208.6	ω_5 (a″)	242.4		
ω_6 (a′)	1628.7	ω_6 (a′)	1631.1	ω_6 (a′)	1627.8		
ω_7 (a′)	3090.3	ω_7 (a′)	3194.0	ω_7 (a′)	3192.7		
ω_8 (a′)	3817.0	ω_8 (a′)	3804.5	ω_8 (a′)	3816.7		
ω_9 (a″)	3941.5	ω_9 (a′)	3935.2	ω_9 (a″)	3942.6		
ZPE	19.45	**ZPE**	18.80	**ZPE**	18.99		

kcal/mol, showing the importance of ZPE and BSSE corrections for weakly interacting systems.

Increasing the symmetry of m1_$^2\Pi$ from C_1 to C_S the ts1_$^2\Pi$ transition state (one imaginary frequency) is obtained, reflecting a pivotal movement of H_2O around the $C \ldots O$ axis [Fig. 1(b)]. The ΔE_0(BSSE)/PMP4-ATZ "interaction" energy is -8.3 kcal/mol, larger by 0.30 kcal/mol than the m1_$^2\Pi$

complex at the same level (Table IV). Obviously, the interaction mechanism of m1_ and ts1_$^2\Pi$ species are identical, but the latter's equilibrium distance $r_{C \ldots O} = 1.792$ Å, is 0.04 Å larger than that of the former.

Figure 3 shows the potential energy curve (PEC) of the m1_$^2\Pi$ HC $\ldots OH_2$ interaction at the MP2/ATZ level, maintaining the equilibrium geometries

TABLE VI _____

Atomic Mulliken charges q and dipole moments μ(Debye) of the $CH(X^2\Pi) \ldots OH_2$ and $CH(a^4\Sigma^-) \ldots OH_2$ complexes at the UMP2/ATZ level[a] (see Fig. 1).

	$CH(^2\Pi) \ldots OH_2$				$CH(^4\Sigma^-) \ldots OH_2$		
	m1_$^2\Pi$	ts1_$^2\Pi$	m2_$^2\Pi$	ts2_$^2\Pi$	m1_$^4\Sigma^-$	ts1_$^4\Sigma^-$	m2_$^4\Sigma^-$
q_C	-0.71	-0.71	-0.50	-0.53	-0.52	-0.45	-0.46
q_{H1}	0.37	0.39	0.48	0.53	0.53	0.44	0.45
q_O	-0.13	-0.17	-0.47	-0.41	-0.43	-0.45	-0.44
q_{H2}	0.22	0.25	0.31	0.20	0.21	0.27	0.22
q_{H3}	0.25	0.25	0.19	0.20	0.21	0.20	0.22
μ	3.955	3.321	3.318	3.763	2.852	2.541	1.836

[a] Mulliken charges and dipole moments of the free CH and H_2O at the UMP2/ATZ level are as follows, $CH(^2\Pi)$: $q_C = -0.42$, $\mu = 1.515$ Debye; $CH(^4\Sigma^-)$: $q_C = -0.44$, $\mu = 0.608$ Debye; H_2O: $q_O = -0.43$, $\mu = 1.859$ Debye.
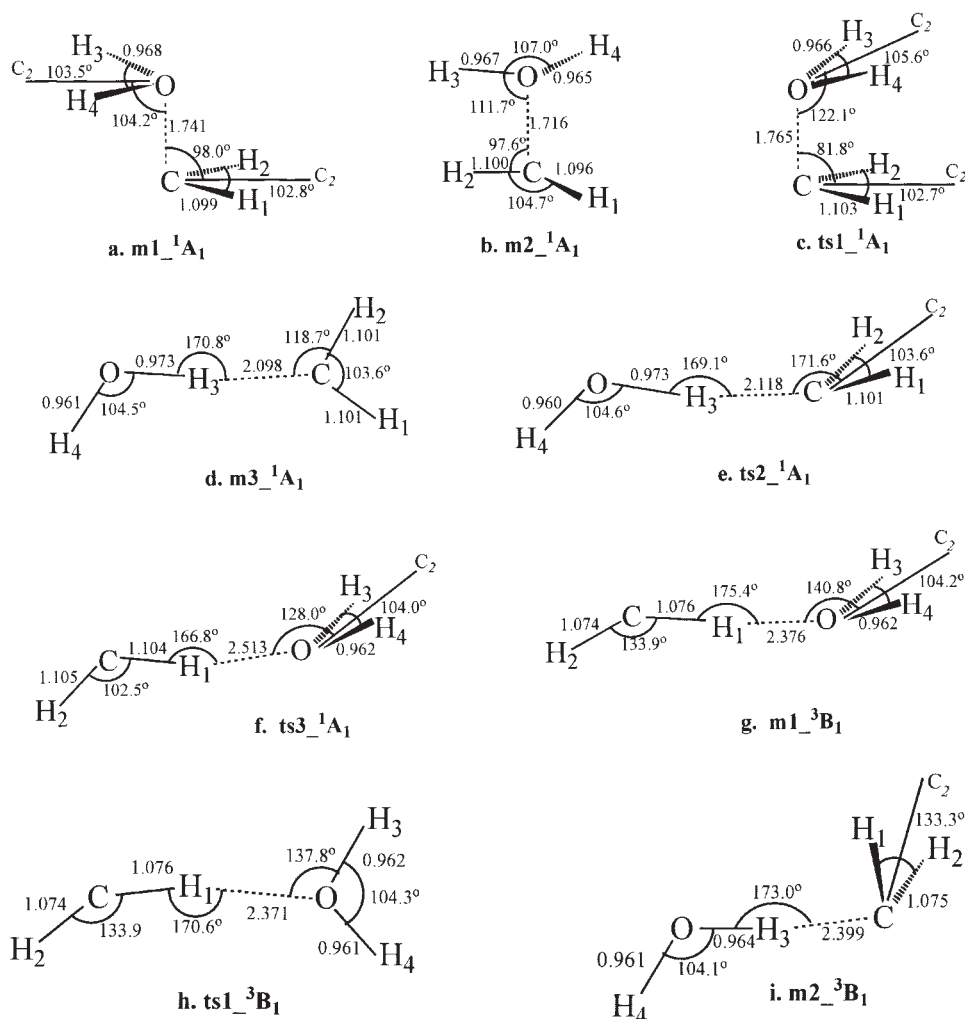
FIGURE 2. Geometries of the CH$_2$($\tilde{a}^1A_1$) . . . OH$_2$ and CH$_2$($\tilde{X}^3B_1$) . . . OH$_2$ minima. Bond distances in Å at the (U)MP2/ATZ level.

of the free CH($X^2\Pi$), H$_2$O fragments along the interaction coordinate.

In both cases m1_$^2\Pi$ and ts1_$^2\Pi$, the bonding is succinctly represented by the vbL diagram shown in Scheme (6), indicating the charge transfer from an oxygen lone pair to the empty $2p_x$-orbital of the CH($X^2\Pi$, B_1 component). Indeed, from the Mulliken population analysis, 0.30 electrons are migrating to the $2p_x$–CH orbital. Note that the H$_1$, C, O, and H$_3$ atoms in m1_$^2\Pi$ [Fig. 1(a)] are practically planar, the dihedral H$_1$COH$_3$ angle being 0.85°. This mechanism suggests that a variety of Lewis bases, L, such as, NH$_3$ and CO, or even noble gases, can form systems of considerable stability with the $X^2\Pi$ CH state.

Finally, the symmetric and asymmetric stretching modes of water in both m1_$^2\Pi$ and ts1_$^2\Pi$ structures are red shifted by 79–97 cm^{-1}, as compared with the free H$_2$O molecule, while the CH stretching is blue shifted by 20 and 43 cm^{-1} in m1_$^2\Pi$ and ts1_$^2\Pi$, respectively (Tables III and V).

The m2_$^2\Pi$ (C_S) and ts2_$^2\Pi$ (C_{2v}) structures constitute the second minimum and second transition state, respectively [Fig. 1(c) and (d)]. At the PMP4/AQZ, we calculate a van der Waals interaction energy for m2_, $\Delta E = -3.78$ kcal/mol, reduced to ΔE_0(BSSE)[CBS] $= -1.94[-1.97]$ kcal/mol, (Table IV) at $r_{C...H} = 2.197$ Å, a significantly high interaction, considering its morphology and the atoms involved. The C_{2v} ts2_$^2\Pi$ van der Waals
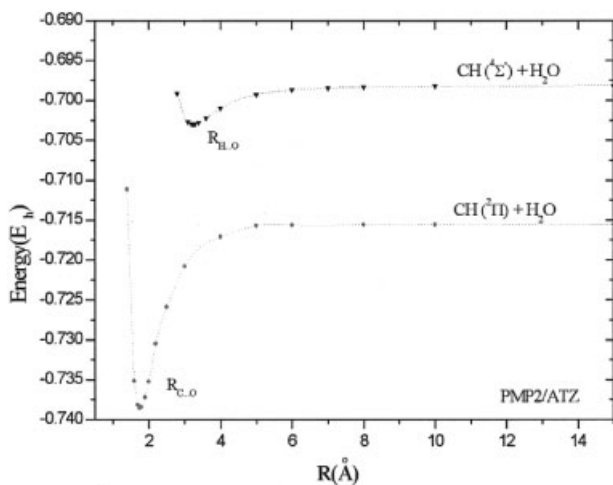
FIGURE 3. Potential energy curves at the UMP2/ATZ level of the m1_$^2\Pi$ CH($^2\Pi$) . . . OH$_2$ and m1_$^4\Sigma^-$ CH($^4\Sigma^-$) . . . OH$_2$ structures.

C—H . . . OH$_2$ PMP4/ATZ interaction is, ΔE = -1.90 kcal/mol reduced to ΔE_0(BSSE) = -0.91 kcal/mol, and estimated to about -1 kcal/mol at the AQZ basis set, using our experience from the m2_$^2\Pi$ interaction. It is interesting that at the AQZ basis set the ts2_$^2\Pi$ structure was calculated to be a real minimum, but at the ATZ level, the previously calculated (ADZ) frequency of 61 cm^{-1} became 20i cm^{-1}. For both m2_$^2\Pi$ and ts2_$^2\Pi$ structures, the C—H bond length decreases by $\sim$0.01 Å upon interaction with water as compared with the free X$^2\Pi$ CH species (Table II). Jursic [7] reports ΔE(MP4SDQ) = -3.4 kcal/mol at $r_{C . . . H}$ = 2.320 Å for the m2_$^2\Pi$ structure; however, this value is reduced to -1.2 kcal/mol if corrected by ZPE and BSSE using our results of the ADZ basis set (Table IV). In addition, concerning the ts2_$^2\Pi$ structure, he concludes that it is a real minimum, although at the MP4SDQ level this configuration is unbound.

Turning now to the CH(a$^4\Sigma^-$) . . . OH$_2$ interaction, we report results for three structures, two minima m1_$^4\Sigma^-$, m2_$^4\Sigma^-$, and one transition state, ts1_$^4\Sigma^-$ [Fig. 1(e), (g) and (f)], all of C$_S$ symmetry. No theoretical results have been reported before in the literature for these systems. The potential energy curve of the m1_$^4\Sigma^-$ along the CH . . . OH$_2$ interaction coordinate constructed as before at the MP2/ATZ level is depicted in Figure 3. Recalling that by singlet coupling two a$^4\Sigma^-$ CH moieties the acetylene molecule is obtained, we expect the CH . . . OH$_2$ interaction to be very similar to the corresponding HCCH . . . OH$_2$ interaction [27]. In-

deed, from Ref. [27] at the MP4/AQZ//MP4/ATZ level, we have ΔE_0(BSSE)[CBS] = $-1.88[-1.92]$ kcal/mol, $r_{HCCH . . . OH_2}$ = 2.188 Å, and φ = 155.8°, while for the m1_$^4\Sigma^-$ at the MP4/AQZ//MP2/ATZ level we obtain ΔE_0(BSSE)[CBS] = $-1.57[-1.69]$ kcal/mol, $r_{CH . . . OH_2}$ = 2.151 Å, and φ = 146.2° [Table IV, Fig. 1(e)]. The C—H bond length within the m1_$^4\Sigma^-$ complex increases by 0.01 Å as contrasted to the free a$^4\Sigma^-$ CH, with a concomitant red shift of the C—H frequency of 116 cm^{-1}.

The interaction energies of m2_$^4\Sigma^-$ and ts1_$^4\Sigma^-$ structures [Fig. 1(g), (f)] at the MP4/AQZ level are ΔE = -0.95 and -1.03 kcal/mol, respectively, but corrected for ZPE and BSSE these values become $+0.2$ and -0.1 kcal/mol, practically unbound.

CH$_2$ . . . OH$_2$

We report six structures of the CH$_2$ (ã$^1A_1$) . . . OH$_2$ complex, three minima (m) and three transition states (ts), and three CH$_2$ (X̃$^3B_1$) . . . OH$_2$ structures, two minima, and one transition state (Fig. 2). Table VII lists absolute energies, BSSE-corrected dissociation energies ΔE(BSSE), and ΔE_0(BSSE); CBS limits are also listed for all five m-structures. Tables VIII and IX give ZPEs and harmonic frequencies, and Mulliken charges and dipole moments, respectively.

The m1_$^1A_1$ (global minimum), m2_$^1A_1$ (second minimum) just 0.3 kcal/mol above the m1_$^1A_1$, and ts1_$^1A_1$ (first transition state) of point group symmetries C$_s$, C$_1$, and C$_s$, respectively, are complexes of ylide character formed by charge transfer of about 0.3 e$^-$ from the oxygen to the empty 2p_x orbital (perpendicular to the CH$_2$ plane) of the ã$^1A_1$ state of methylene [see also Scheme (4)]. The vbL diagram shown in Scheme 7 clearly captures the physics of bonding.

The interaction energies ΔE with respect to CH$_2$ (ã$^1A_1$) + H$_2$O at the MP4/AQZ//MP2/ATZ are -15.72 and -15.45 kcal/mol for the m1_$^1A_1$ and m2_$^1A_1$, respectively. Correcting these values for ZPE and BSSE, we obtain ΔE_0(BSSE) = -9.31 and -8.99 kcal/mol (Table VII). The final interaction energy of the global minimum m1_$^1A_1$ at the CBS limit is -9.73 kcal/mol. Assuming a similar CBS correction for the second minimum (m2), one estimates its interaction energy to be -9.4 kcal/mol.

The corresponding values for the ts1_$^1A_1$ structure at the MP4/ATZ//MP2/ATZ level are ΔE = -10.52 kcal/mol, ΔE_0(BSSE) = -4.07 kcal/mol, or

TABLE VII _____

Total energies E (hartree), interaction energies ΔE (kcal/mol), basis set superposition error-corrected ΔE, ΔE(BSSE) (kcal/mol), and zero-point energy-corrected ΔE(BSSE), ΔE_0(BSSE) (kcal/mol), of CH$_2$(ã^{1}A$_1$, X̃^{3}B$_1$) . . . OH$_2$ complexes at different levels of theory.

	E	ΔE	ΔE(BSSE)	ΔE_0(BSSE)	E	ΔE	ΔE(BSSE)	ΔE_0(BSSE)
			ADZ					
			(U)MP2[a]				(U)MP4[a]	
m1_^{1}A$_1$	−115.28599	−15.76	−13.24	−7.46	−115.32511	−14.47	−12.00	−6.22
ts1_^{1}A$_1$	−115.27810	−10.81	−8.51	−3.29	−115.31775	−9.58	−7.60	−2.38
m3_^{1}A$_1$	−115.27052	−6.06	−5.13	−2.84	−115.31123	−5.76	−4.84	−2.55
ts2_^{1}A$_1$	−115.27026	−5.89	−4.98	−2.78	−115.31099	−5.61	−4.69	−2.50
ts3_^{1}A$_1$	−115.26357	−1.70	−1.23	−0.27	−115.30474	−1.69	−1.19	−0.23
m1_^{3}B$_1$	−115.28930	−1.95	−1.42	−0.24	−115.32441	−2.07	−1.48	−0.30
ts1_^{3}B$_1$	−115.28916	−1.87	−1.36	−0.45	−115.32424	−1.97	−1.41	−0.50
m2_^{3}B$_1$	−115.28905	−1.80	−1.23	−0.11	−115.32416	−1.92	−1.29	−0.18
			PMP2				PMP4	
m1_^{3}B$_1$	−115.29114	−1.96	−1.43	−0.25	−115.32555	−2.07	−1.48	−0.30
ts1_^{3}B$_1$	−115.29100	−1.88	−1.37	−0.46	−115.32538	−1.97	−1.41	−0.50
m2_^{3}B$_1$	−115.29088	−1.80	−1.23	−0.11	−115.32530	−1.92	−1.29	−0.17
			ATZ					
			(U)MP2[a]				(U)MP4[a,b]	
m1_^{1}A$_1$	−115.39070	−17.13	−16.06	−10.04	−115.42916	−15.49	−14.50	−8.48
m2_^{1}A$_1$	−115.39061	−17.07	−15.95	−9.89	−115.42869	−15.20	−14.16	−8.10
ts1_^{1}A$_1$	−115.38243	−11.94	−10.92	−5.42	−115.42123	−10.52	−9.57	−4.07
m3_^{1}A$_1$	−115.37311	−6.09	−5.69	−3.39	−115.41377	−5.84	−5.46	−3.17
ts2_^{1}A$_1$	−115.37284	−5.92	−5.52	−3.32	−115.41351	−5.67	−5.30	−3.10
ts3_^{1}A$_1$	−115.36600	−1.63	−1.39	−0.51	−115.40704	−1.61	−1.37	−0.49
m1_^{3}B$_1$	−115.38942	−1.79	−1.54	−0.44	−115.42509	−1.89	−1.63	−0.53
ts1_^{3}B$_1$	−115.38929	−1.70	−1.49	−0.64	−115.42492	−1.78	−1.57	−0.72
m2_^{3}B$_1$	−115.38934	−1.73	−1.47	−0.31	−115.42501	−1.84	−1.58	−0.42
			PMP2				PMP4	
m1_^{3}B$_1$	−115.39132	−1.80	−1.55	−0.45	−115.42620	−1.88	−1.62	−0.53
ts1_^{3}B$_1$	−115.39118	−1.71	−1.50	−0.65	−115.42604	−1.77	−1.56	−0.72
m2_^{3}B$_1$	−115.39122	−1.74	−1.48	−0.32	−115.42613	−1.83	−1.57	−0.41
			AQZ[c]					
			(U)MP2[a]				(U)MP4[a]	
m1_^{1}A$_1$	−115.42424	−17.30	−16.79	−10.77	−115.45938	−15.72	−15.33	−9.31
CBS[d]			−17.05 ± 0.02				−15.75 ± 0.02	
m2_^{1}A$_1$	−115.42418	−17.27	−16.73	−10.67	−115.45896	−15.45	−15.05	−8.99
m3_^{1}A$_1$	−115.40624	−6.01	−5.82	−3.52	−115.44351	−5.75	−5.61	−3.31
CBS[d]			5.86				−5.66	
m1_^{3}B$_1$	−115.42152	−1.70	−1.59	−0.49	−115.45431	−1.79	−1.70	−0.60
CBS[d]			−1.64				−1.75	
m2_^{3}B$_1$	−115.42140	−1.62	−1.51	−0.35	−115.45420	−1.72	−1.63	−0.47
			−1.52				−1.64	
			PMP2				PMP4	
m1_^{3}B$_1$	−115.42342	−1.71	−1.60	−0.50	−115.45542	−1.78	−1.69	−0.59
CBS[d]			−1.64				−1.76	
m2_^{3}B$_1$	−115.42329	−1.62	−1.52	−0.36	−115.45531	−1.71	−1.63	−0.47
CBS[d]			−1.52				−1.64	

[a] For the CH$_2$(^{1}A$_1$) . . . OH$_2$ the UMP2 and UMP4 is MP2 and MP4, respectively.
[b] (U)MP4/ATZ//(U)MP2/ATZ.
[c] (U)MP2, (U)MP4/AQZ//(U)MP2/ATZ.
[d] Complete basis set limit.

TABLE VIII

MP2/ATZ harmonic vibrational frequencies $\omega(cm^{-1})$ and zero-point energies ZPE (kcal/mol) of the $CH_2(\tilde{a}^1A_1) \ldots OH_2$ (m1, m2, ts1, m3, ts2, ts3) and $CH_2(\tilde{X}^3B_1) \ldots OH_2$ (m1, ts1, m2) complexes.

m1_$^1A_1$		m2_$^1A_1$		ts1_$^1A_1$		m3_$^1A_1$		ts2_$^1A_1$	
ω_1 (a″)	101	ω_1	150	ω_1 (a″)	343i	ω_1 (a″)	86.6	ω_1(a″)	86.2i
ω_2 (a′)	442	ω_2	442	ω_2 (a′)	388	ω_2 (a′)	138	ω_2(a″)	145
ω_3 (a″)	695	ω_3	662	ω_3 (a′)	654	ω_3 (a″)	187	ω_3(a′)	166
ω_4 (a′)	710	ω_4	730	ω_4 (a″)	703	ω_4 (a″)	208	ω_4(a′)	225
ω_5 (a″)	1183	ω_5	1149	ω_5 (a″)	1164	ω_5 (a′)	403	ω_5(a′)	498
ω_6 (a′)	1186	ω_6	1201	ω_6 (a′)	1182	ω_6 (a″)	727	ω_6(a″)	640
ω_7 (a′)	1423	ω_7	1423	ω_7 (a′)	1390	ω_7 (a′)	1423	ω_7(a′)	1423
ω_8 (a′)	1655	ω_8	1614	ω_8 (a′)	1611	ω_8 (a′)	1656	ω_8(a′)	1658
ω_9 (a′)	3006	ω_9	3008	ω_9 (a′)	2964	ω_9 (a′)	3021	ω_9(a′)	3021
ω_{10} (a″)	3080	ω_{10}	3100	ω_{10} (a″)	3045	ω_{10} (a′)	3103	ω_{10}(a″)	3103
ω_{11} (a′)	3751	ω_{11}	3755	ω_{11} (a′)	3746	ω_{11} (a′)	3619	ω_{11}(a′)	3627
ω_{12} (a″)	3848	ω_{12}	3877	ω_{12} (a″)	3875	ω_{12} (a′)	3906	ω_{12}(a′)	3907
ZPE	30.14	**ZPE**	30.18	**ZPE**	29.62	**ZPE**	26.42	**ZPE**	26.32

ts3_$^1A_1$		m1_$^3B_1$		ts1_$^3B_1$		m2_$^3B_1$	
ω_1 (a″)	101.3i	ω_1 (a″)	63.2	ω_1 (a″)	66.2i	ω_1 (a″)	39.1
ω_2 (a′)	65.0	ω_2 (a″)	70.3	ω_2 (a″)	10.6	ω_2 (a″)	81.6
ω_3 (a″)	75.5	ω_3 (a′)	81.5	ω_3 (a′)	59.9	ω_3 (a′)	94.0
ω_4 (a′)	95.6	ω_4 (a′)	107	ω_4 (a′)	106	ω_4 (a′)	122
ω_5 (a″)	165	ω_5 (a′)	175	ω_5 (a′)	205	ω_5 (a′)	228
ω_6 (a′)	196	ω_6 (a″)	310	ω_6 (a″)	238	ω_6 (a″)	312
ω_7 (a′)	1427	ω_7 (a′)	1132	ω_7 (a′)	1135	ω_7 (a′)	1134
ω_8 (a′)	1632	ω_8 (a′)	1629	ω_8 (a′)	1629	ω_8 (a′)	1631
ω_9 (a′)	2995	ω_9 (a′)	3181	ω_9 (a′)	3183	ω_9 (a′)	3194
ω_{10} (a′)	3074	ω_{10} (a′)	3419	ω_{10} (a′)	3421	ω_{10} (a″)	3428
ω_{11} (a′)	3818	ω_{11} (a′)	3819	ω_{11} (a′)	3820	ω_{11} (a′)	3787
ω_{12} (a″)	3941	ω_{12} (a″)	3943	ω_{12} (a″)	3945	ω_{12} (a′)	3923
ZPE	24.99	**ZPE**	25.63	**ZPE**	25.38	**ZPE**	25.69

estimated to be about -5 kcal/mol at the CBS limit, judging from our previous experience.

The ts1_$^1A_1$ structure is the transition state between two energetically equivalent m2_$^1A_1$ structures with respect to the pivotal movement of the H_2O molecule around the C . . . O axis of m2_$^1A_1$ [Fig. 2(b)], meaning that the energy barrier of this librational motion is 4.0 kcal/mol at the MP4/ATZ level. Figure 4 depicts the MP4/ATZ PEC of CH_2 $(\tilde{a}^1A_1)$ + H_2O along the C . . . O coordinate. Finally, in all three structures, the symmetric and asymmetric stretching of water is red shifted ~70–100 cm^{-1} and the methylene bending are red shifted by 50–80 cm^{-1}.

The previous theoretical literature concerning the m1_$^1A_1$ CH_2 . . . OH_2 complex is significant [14–

20] (see Table I). Although, in general, all previous works give the m1_$^1A_1$ conformation as a minimum, the level of calculations are considerably lower than the present one and lacking systematic BSSE + ZPE corrections. This is reflected in a variety of conflicting results. For instance, the interaction energy of C . . . O ranges from -5.91 [18] to -20.14 [17] kcal/mol, or corrected for ZPE, -15.3 [20] to -2.89 [18] kcal/mol. Similarly, C . . . O distances range from 1.758 [20] to 2.366 Å. [18] The m2_$^1A_1$ structure was also examined in 1996 [21] at the MP2 and QCISD(T) + ZPE level, giving $\Delta E_0 = -9.30$ (MP2) and -6.37 [QCISD(T)] kcal/mol.

The rest of the $CH_2(\tilde{a}^1A_1)$ . . . OH_2 structures presently studied and shown in Figure 2 are a third minimum (m3_$^1A_1$) and two transition structures
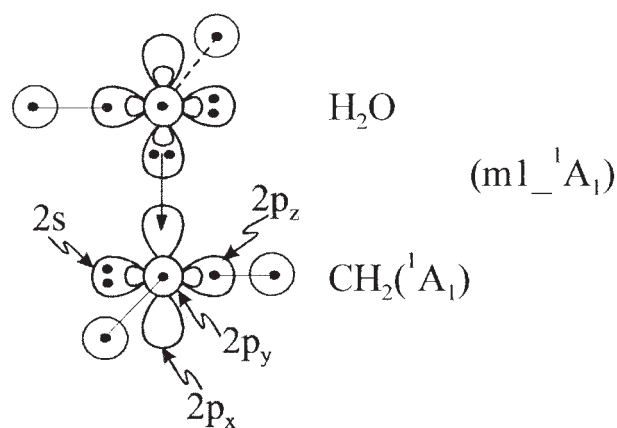
TABLE IX _____

Atomic Mulliken charges q and dipole moments μ (Debye) of the CH_2($\tilde{a}^1A_1$) ... OH_2 and CH_2($\tilde{X}^3B_1$) ... OH_2 complexes at the (U)MP2/ATZ level.[a]

	CH_2($\tilde{a}^1A_1$) ... H_2O					
	m1_$^1A_1$	m2_$^1A_1$	ts1_$^1A_1$	m3_$^1A_1$	ts2_$^1A_1$	ts3_$^1A_1$
q_C	−0.99	−0.99	−0.88	−0.87	−0.86	−0.85
q_{H1}	0.33	0.34	0.30	0.46	0.42	0.49
q_{H2}	0.33	0.31	0.30	0.40	0.42	0.37
q_O	−0.13	−0.10	−0.14	−0.48	−0.47	−0.42
q_{H3}	0.23	0.19	0.21	0.30	0.30	0.21
q_{H4}	0.23	0.25	0.21	0.19	0.19	0.21
μ	3.403	4.193	4.904	3.692	3.669	2.251
	CH_2($\tilde{X}^3B_1$) ... H_2O					
	m1_$^3B_1$	ts1_$^3B_1$	m2_$^3B_1$	ts2_$^3B_1$		
q_C	−1.00	−1.01	−0.89	−0.93		
q_{H1}	0.58	0.58	0.44	0.46		
q_{H2}	0.43	0.43	0.44	0.46		
q_O	−0.43	−0.41	−0.47	−0.42		
q_{H3}	0.21	0.19	0.27	0.21		
q_{H4}	0.21	0.21	0.20	0.21		
μ	2.080	2.312	1.776	2.632		

[a] Mulliken charges and dipole moments of the free CH_2 and H_2O at the (U)MP2/ATZ level are as follows: CH_2($\tilde{a}^1A_1$): $q_C = -0.80$, $\mu = 1.814$ Debye; CH_2($\tilde{X}^3B_1$): $q_C = -0.91$, $\mu = 0.594$ Debye; H_2O: $q_O = -0.43$, $\mu = 1.859$ Debye.

(ts2_ and ts3_$^1A_1$), all belonging to the C_S point group. The ts2_$^1A_1$ is the transition state between two (energetically) equivalent m3_$^1A_1$ structures with a very small energy barrier (<0.2 kcal/mol, including ZPE corrections). At the MP4/AQZ// MP2/ATZ level, the m3_$^1A_1$ C ... H interaction energy amounts to $\Delta E = -5.75$ kcal/mol or ΔE_0(BSSE)[CBS] $= -3.31[-3.36]$ kcal/mol, and practically the same in the ts2_$^1A_1$. It is interesting to observe that we are dealing with a remarkably strong (-3.4 kcal/mol) C ... H "hydrogen bond" in both m3_ and ts2_$^1A_1$ structures, probably the result of the positive end of the water hydrogen [H_3 in Fig. 1(d)] facing the cylindrically symmetric 2s (or $2sp_z$ hybrid) of the CH_2 $\tilde{a}^1A_1$ state [Scheme (8)].
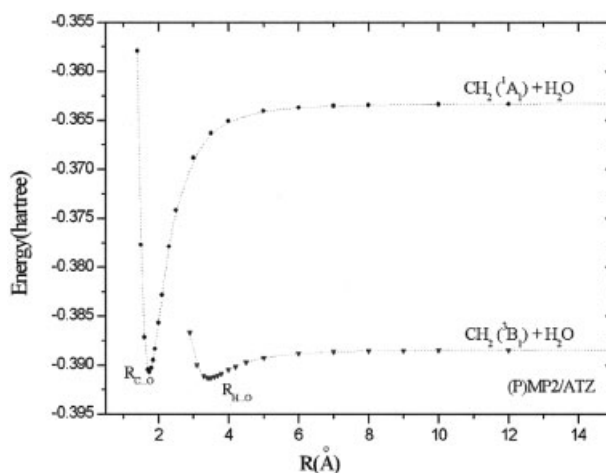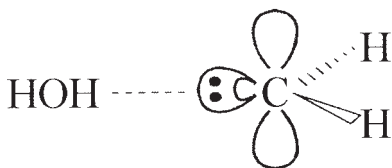

SCHEME 7.

FIGURE 4. Potential energy curves at the (U)MP2/ATZ level of the m1_$^1A_1$ CH_2($\tilde{a}^1A_1$) ... OH_2 and m1_$^3B_1$ CH_2($\tilde{X}^3B_1$) ... OH_2 structures.

SCHEME 8.

Finally, and in accordance with the previously discussed strong $C \ldots HOH$ interaction, a red shifted $O\!-\!H$ stretching interaction of ~ 200 cm^{-1} is calculated for both m3_ and ts2_^{1}a$_1$ structures. The ts3_^{1}A$_1$ transition state [Fig. 1(f)] concerns a $CH \ldots O$ interaction with $\Delta E[\Delta E_0(\text{BSSE})] = -1.61[-0.49]$ kcal/mol.

We discuss now the interaction of H_2O with the $\tilde{X}^3B_1$ state of CH_2. Looking at the electronic distribution of the $\tilde{X}^3B_1$ [Scheme (5)], we expect weak van der Waals interactions between these two species, and indeed this is the case. No calculations have been reported so far on the $\tilde{X}^3B_1$ state of $CH_2 + H_2O$.

We present results for two minima (m1_^{3}B$_1$, m2_^{3}B$_1$) and one transition state (ts1_^{3}B$_1$), all of geometrical C_s symmetry [Fig. 2(g), (h), and (i)]. The $H \ldots O$ interaction energy of m1_^{3}B$_1$ is $\Delta E = -1.78$ kcal/mol at the MP4/AQZ//MP2/ATZ, or including ZPE and BSSE corrections, $\Delta E_0(\text{BSSE})[\text{CBS}] = -0.59[-0.66]$ kcal/mol (Table VII). Figure 4 shows the PMP2/ATZ potential curve of m1_^{3}B$_1$ along the $H \ldots O$ coordinate.

The ts1_^{3}B$_1$ is the transition state between two equivalent (mirror images) geometries of m1_^{3}B$_1$, but the total energy differences between the m1_^{3}B$_1$ and ts1_^{3}B$_1$ is negligible, making the two structures practically indistinguishable. Contrasting the total energies of m1_^{1}A$_1$ and m1_^{3}B$_1$ corrected for ZPE, BSSE and including the CBS limit at MP4/AQZ level, it is seen (Tables II, III, and VII) that the global minimum of the $CH_2 \ldots OH_2$ complex is the m1_^{3}B$_1$ state by -1.97 kcal/mol. However, considering our MP4/AQZ $\tilde{a}^1A_1 \leftarrow \tilde{X}^3B_1$ energy splitting of 11.04 kcal/mol (Tables II and III), larger by 2.0 kcal/mol from the experimental value [26], we can claim with confidence that the m1_^{1}A$_1$ and m1_^{3}B$_1$ states are in essence degenerate. Lastly, in the m2_^{3}B$_1$, at the MP4/AQZ//MP2/ATZ level, the $H \ldots C$ interaction energy is $\Delta E = -1.71$ kcal/mol, reduced to -0.47 kcal/mol by adding the ZPE and BSSE corrections, or -0.48 kcal/mol at the CBS limit (Table VII).

Synopsis

Employing the (P)MP$n(n = 2, 4)$ technique in conjunction with the sequence of correlation consistent basis sets aug-cc-pVxZ, $x = 2$, 3, and 4, we have systematically examined the weakly interacting systems $CH(X^2\Pi, a^4\Sigma^-) + H_2O$ and $CH_2(\tilde{X}^3B_1, \tilde{a}^1A_1) + H_2O$. For the $CH \ldots OH_2$ system, we have located four minima (m) and three transition states (ts, one imaginary frequency), and five minima and four transition states for the $CH_2 \ldots OH_2$. All our results have been corrected for ZPE and BSSE, while for the most important m_ structures, we report complete basis set (CBS) interaction limits.

The highest $CH(X^2\Pi) \ldots OH_2$ [m1_$^2\Pi$, Fig. 1(a)] and $CH_2(\tilde{a}^1A_1) \ldots OH_2$ [m1_^{1}A$_1$; Fig. 2(a)] interactions are the result of electron transfer from the oxygen atom to the empty p_π orbitals of $CH(X^2\Pi)$ and $CH_2(\tilde{a}^1A_1)$, respectively. Specifically, and at the highest level of calculation (P)MP4/AQZ//MP2/ATZ, including ZPE, BSSE, and CBS extrapolation, we obtain $\Delta E_0(\text{BSSE}) + \text{CBS} = -9.36$ kcal/mol at $r_{C \ldots O} = 1.752$ Å, and -9.73 kcal/mol at $r_{C \ldots O} = 1.741$ Å for m1_$^2\Pi$ and m1_^{1}A$_1$, respectively. The obvious similarity of the interaction mechanism causes practically the same "binding energies" and bond distances for both systems.

In the m1_$^4\Sigma^-$ $CH \ldots H_2O$ complex [Fig. 1(e)], we obtain $\Delta E_0(\text{BSSE}) + \text{CBS} = -1.69$ kcal/mol at $r_{H \ldots O} = 2.151$ Å, close to the corresponding $HC\!\equiv\!CH \ldots OH_2$ interaction [27], as expected.

Furthermore, in the $CH_2 \ldots H_2O$ complex, the m3_^{1}A$_1$ structure [Fig. 2(d)] has a remarkably strong $C \ldots H$ "hydrogen bond," $\Delta E_0(\text{BSSE}) + \text{CBS} = -3.36$ kcal/mol at $r_{H \ldots C} = 2.098$ Å, while the m1_^{3}B$_1$ species [Fig. 2(g)] gives a $\Delta E_0(\text{BSSE}) + \text{CBS} = -0.66$ kcal/mol at $r_{H \ldots O} = 2.376$ Å.

Finally, the global minimum of the $CH_2 \ldots OH_2$ complex is the m1_^{3}B$_1$ state, lower than m1_^{1}A$_1$ by 1.97 kcal/mol. However, considering our MP4/AQZ $\tilde{a}^1A_1 \leftarrow \tilde{X}^3B_1$ energy splitting of 11.04 kcal/mol, 2.0 kcal/mol larger than the experimental value [30f], we conclude that m1_^{1}A$_1$ and m1_^{3}B$_1$ states are in essence degenerate.

References

1. Padwa, A.; Hornbuckle, S. F. Chem Rev 1991, 91, 263.

2. Streitwieser, A., Jr.; Heathcock, C. H. Introduction to Organic Chemistry, 3rd ed.; Macmillan, New York, 1985.

3. Sanders, W. A.; Lin, M. C. Chemical Kinetics of Small Organic Radicals; Afassi, Z., Ed.; CRC Press: Boca Raton, FL, 1988; Vol III.

4. Zabarnick, S.; Fleming, J. W.; Lin, M. C. Chem Phys 1989, 132, 407.

5. Hou, Z.; Bayes, K. D. J Phys Chem 1993, 97, 1896.

6. Wang, Z.-X.; Liu, R.-Z.; Huang, M.-B.; Yu, Z. Can J Chem 1996, 74, 910.

7. Jursic, B. S. J Phys Chem 1998, 102, 9255.

8. Ma, S.-Y.; Liu, R.-Z. Huaxue Xuebao 1996, 54, 632.

9. Kalemos, A.; Dunning, T. H., Jr.; Mavridis, A.; Harrison, J. F. Can J Chem 2004, 82, 684.

10. Wesdemiotis, C.; Feng, R.; Danis, P. O.; Williams, E. R.; McLafferty, F. W. J Am Chem Soc 1986, 108, 5847.

11. Hack, W.; Wagner, H. G.; Wilms, A. Ber Bunsenges Phys Chem 1988, 92, 620.

12. Cartensen, H.-H.; Wagner, H. G. Ber Bunsenges Phys Chem 1995, 99, 1539.

13. Staker, W. S.; King, K. D.; Gutsche, G. J.; Lawrance, W. D. J Chem Soc Faraday Trans 1991, 87, 2421.

14. Harding, L. B.; Schlegel, H. B.; Krishnan, R.; Pople, J. A. J Phys Chem 1980, 84, 3394.

15. Eades, R. A.; Gassman, P. G.; Dixon, D. A. J Am Chem Soc 1981, 103, 1066.

16. Pople, J. A.; Raghavachari, K.; Frisch, M. J.; Binkley, J. S.; Schleyer, P. v. R. J Am Chem Soc 1983, 105, 6389.

17. Yates, B. F.; Bouma, W. J.; Radom, L. J Am Chem Soc 1987, 109, 2250.

18. Walch, S. P. J Chem Phys 1993, 98, 3163.

19. Zub, L. L.; Standard, J. M. J Mol Struct 1996, 368, 133.

20. Tucker, J. M.; Standard, J. M. J Mol Struct 1998, 431, 193.

21. Gonzalez, C.; Restrepo-Cossio, A.; Marquez, M.; Wiberg, K. B. J Am Chem Soc 1996, 118, 5408.

22. (a) Dunning, T. H., Jr. J Chem Phys 1989, 90, 1007; (b) Kendall, R. A.; Dunning, T. H., Jr.; Harrison, R. J. J Chem Phys 1992, 96, 6796.

23. (a) Frisch, M. J.; Trucks, G. W.; Schlegel, H. B.; Gill, P. M. W.; Johnson, B. G.; Robb, M. A.; Cheeseman, J. R.; Keith, T. A.; Peterson, G. A.; Montgomery, J. A.; Raghavachari, K.; Al-Laham, M. A.; Zakrzewski, V. G.; Ortiz, J. V.; Foresman, J. B.; Cioslowski, J.; Stefanov, B. B.; Nanayakkara, A.; Challacombe, M.; Peng, C. Y.; Ayala, P. Y.; Chen, W.; Wong, M. W.; Andres, J. L.; Replogle, E. S.; Gomperts, R.; Martin, R. L.; Fox, D. J.; Binkley, J. S.; Defrees, D. J.; Baker, J.; Stewart, J. P.; Head-Gordon, M.; Gonzalez, C.; Pople, J. A. Gaussian 94, Revision A.1; Gaussian: Pittsburgh, PA, 1994; (b) Gaussian 98; Gaussian: Pittsburgh, PA, 1998.

24. (a) Boys, S. F.; Bernardi, F. Mol Phys 1970, 19, 553; (b) Davidson, E. R.; Chakravorty, S. J Chem Phys Lett 1994, 217, 48.

25. (a) Van Duijneveldt, F. B.; van Duijneveldt-van de Rijdt, J. G. C. M.; van Lenthe, J. H. Chem Rev 1994, 94, 1873; (b) Jeziorski, B.; Moszynski, R.; Szalewicz, K. Chem Rev 1994, 94, 1887.

26. Xantheas, S. S. J Chem Phys 1996, 104, 8821.

27. Tzeli, D.; Mavridis, A.; Xantheas, S. J Chem Phys 2000, 112, 6178; J Phys Chem A 2002, 106, 11327.

28. See, e.g., Peterson, K. A.; Dunning, T. H., Jr. J Mol Struct (Theochem) 1997, 400, 93.

29. (a) Huber, K. P.; Herzberg, G. Constants of Diatomic Molecules; Van Nostrand Reinhold: New York, 1979; (b) Zachwieja, M. J Mol Spectrosc 1995, 170, 285; (c) Kasdan, A.; Herbst, E.; Lineberger, W. C. Chem Phys Lett 1975, 31, 78; (d) Nelis, T.; Brown, J. M.; Evenson, K. M. J Chem Phys 1988, 88, 2087; J Chem Phys 1990, 92, 4067.

30. (a) Herzberg, G.; Johns, J. W. C. Proc R Soc London Ser A 1966, 295, 107; (b) Leopold, D. G.; Murray, K. K.; Stevens Miller, A. E.; Lineberger, W. C. J Chem Phys 1985, 83, 4849; (c) Peterson, K. A.; Dunning, T. H., Jr. J Chem Phys 1997, 106, 4119; (d) McKellar, A. R. W.; Bunker, P. R.; Sears, T. J.; Evenson, K. M.; Saykally, R. J.; Langhoff, S. R. J Chem Phys 1983, 89, 5251; (e) Bunker, P. R.; Jensen, P.; Kraemer, W. P.; Beardsworth, R. J Chem Phys 1985, 85, 3724; (f) Bunker, P. R.; Jensen, P. J Chem Phys 1988, 89, 1327; (g) Császár, A. G.; Leininger, M. L.; Szalay, V. J Chem Phys 2003, 118, 10631.

31. (a) Cook, R. L.; De Lucia, F. C.; Helminger, P. J Mol Spectrosc 1974, 53, 62; (b) Hoy, A. R.; Bunker, P. R. J Mol Spectrosc 1974, 52, 439; J Mol Spectrosc 1975, 59, 159; (c) Benedict, W. S.; Gailar, N.; Plyler, E. K. J Chem Phys 1956, 24, 1139.

32. Kalemos, A.; Mavridis, A.; Metropoulos, A. J Chem Phys 1999, 111, 9536.